Mission Analyses for Low-Earth-Observation Missions with Spacecraft Formations

Prof. Dr. Klaus Schilling
Chair Robotics and Telematics
Julius-Maximilians-University Würzburg
Am Hubland
D-97074 Würzburg
GERMANY

schi@informatik.uni-wuerzburg.de

ABSTRACT

The orbit properties for Earth observation missions will be reviewed, addressing Sun and Earth synchronous orbits as well as the determination of ground tracks, eclipse periods, ground station contact durations, surface visibility conditions. These properties for single spacecraft will be expanded to multiple distributed satellite systems. With respect to Earth observation such formations and constellations of satellites are used to achieve an improved temporal and spatial resolution for observations, in addition to higher responsiveness, robustness and graceful degradation in case of defects. Telecommunication links between the spacecrafts and towards the ground stations to form a mobile ad-hoc sensor network are analyzed.

1.0 INTRODUCTION

Distributed systems of small satellites offer interesting capabilities to complement traditional Earth observation satellites with respect to increasing temporal and spatial resolution. Observations of surface points from different viewing angles at very long baselines provide the potential for data fusion to derive 3-D-images.

Groups of satellites are described as:

- ***Constellation***, when several satellites flying in similar orbits without control of relative position, are organized in time and space to coordinate ground coverage. They are controlled separately from ground control stations.
- ***Formation***, if multiple satellites with closed-loop control on-board provide a coordinated motion control on basis of relative positions to preserve an appropriate topology for observations. Several spacecrafts coordinate to perform the function of a single, large, virtual instrument.
- ***Swarm*** or ***Cluster,*** if a distributed system of similar spacecraft is cooperating to achieve a joint goal without fixed absolute or relative positions. Each member determines and controls relative positions to the other satellites.

Examples for typical constellations are provided in different application fields, such as navigation (GPS, GLONASS, Galileo), telecommunication (TDRSS, Iridium, Globalstar, Orbcomm, Teledesic), remote sensing (Rapid Eye). With respect to formations, an example is provided by ESA's CLUSTER mission to measure the 3-D-structure of the Earth's magnetic field by a pyramidal shaped formation of satellites, or by ESA's DARWIN mission to point synchronously five free flying telescopes towards one target point in order to achieve enough resolution to detect planets in remote solar systems (for further details see www.esa.int). Formations thus enable higher resolution imagery and interferometry.

For the self-organisation in groups essential ingredients are communication and control strategies. The system capabilities can be significantly increased by an appropriate combination of data from multiple cooperating technical components. Therefore in this article the orbit properties, and in addition also the flow of information between satellites by mobile ad-hoc networks (MaNets) and coordination of swarms are addressed. Similar to applications with terrestrial vehicles generic properties of sensor networks, including groups of mobile observation and measurement stations (such as aircraft, submarines or robotic cars) are addressed. Space applications rise additional challenges such as significant delays in the telecommunication link due to large distances, high dynamics in changing positions and high levels of noise effects.

The use of satellite swarms provides interesting innovative contributions to Earth surface monitoring. While there is increasing demand for border surveillance and environment pollution monitoring, currently related satellite missions are mainly based on single large satellites and only few on simple satellite constellations (such as Rapid Eye). For emergencies, the traditional systems do not achieve the desirable spatial and temporal resolution needed to characterize the situation in almost real-time. The use of satellite swarms offers an interesting complementary approach. In particular swarms composed of pico-satellites promise a long term perspective for a quick, event based and scalable provision of Earth observation capacities from a low Earth orbit (LEO). Such networks of satellites offer fault-tolerant performance with graceful degradation in case of defects. On the other side each spacecraft needs a sensor and control system to maintain a required relative position and attitude to the other satellites.

For coordinated multi-satellite Earth observations, so far mainly tandem missions by two satellites were used, such as ERS-1 / ERS-2, or Landsat / EO-1. A formation of four satellites for measurement of the Earth's magnetic field provided Cluster / Phoenix. All spacecraft were directly controlled from ground, the coordination of this configuration occurred by interaction between the ground controllers. Thus in particular for the application areas of Earth observation, for the observation of physical properties of the space environment, and for astronomical measurements, there is an obvious demand for software to increase automation and to support control of larger configurations of satellites.

In the field of telecommunication and navigation applications, there exist operational satellite constellations as pointed out before, but all are controlled directly from ground and active measurements on-board the satellites for configuration management are not yet performed (Alfriend et. al., 2010).

Other interesting trends supporting formations are related to miniaturization techniques and in distributed information systems to realize such small satellite. The University Würzburg supports the program UWE (***U***niversity ***W***ürzburg's ***E***xperimental satellites) related to development of thee technology base for coordinated, distributed pico-satellites (satellites with a mass of about 1 kg). The pico-satellite UWE-1 has been launched on 27.10.2005 and performed in orbit successful telecommunication experiments on optimization of parameters in the Internet-Protocol (IP) according to the space environment [Schilling, 2006]. The objective of UWE-2 is related to attitude determination by fusing data from GPS, gyros, sun sensors and accelerometers [Schmidt et al., 2008]. It was launched in September 2009. Currently UWE-3 is under development to demonstrate miniaturized actuators for attitude control. Due to the miniaturization needed to realize such pico-satellites in the 1 kg-class, the performance is limited in comparison to traditional satellites. Nevertheless by sensor data fusion of multiple pico-satellites this should be compensated. By use of modern information processing methods, there can fault tolerant, scalable systems be realized, offering in space applications innovative perspectives for applications in environment monitoring and telecommunications.

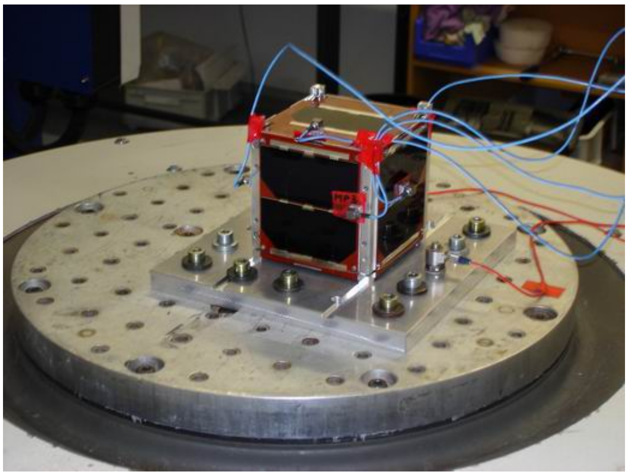

Figure 1: Prototype of UWE-1 during vibration tests.

An infrastructure to efficiently control a group of satellites from ground is currently only in first approaches realized, decentralized approaches [Scharf et al.,2004; Murphy/Pardalos, 2000] are not yet implemented. Challenging technologies to be implemented for distributed small satellite systems include:

- *Determination of attitude and position*: miniaturized sensors are to be introduced to determine the attitude of the satellite with sufficient accuracy for the interpretation of measurements, as well as for the relative distance determination between the spacecrafts.
- *Autonomous control of position and attitude*: the deviation between measured position and attitude towards target values is to be determined in order to generate related correction maneuvers. In orbit there is only sporadic contact to ground control stations, thus real-time reaction capabilities are to be implement.
- *Operations of satellite swarms:* the control of satellite formations requires the coordination of autonomous reaction capabilities on-board with ground control interactions, characterized by signal propagation delays and link interrupts. The operator would benefit from functions, enabling just to control a leader satellite, while at a given formation the trajectories of the others are generated autonomously.

2.0 MISSION ANALYSIS FOR EARTH OBSERVATION SATELLITES

Typical orbits for Earth observation satellites are discussed in this section. Orbits of satellites in a point-mass gravitational field are Kepler orbits, e.g. ellipsoids for closed trajectories. In this context an orbit around the Earth can be described in terms of the Kepler parameters (five fixed parameters and one variable changing with time):

a - semi-major axis (size of the ellipse)
ε - eccentricity ("flatness" of the ellipse)
i - inclination (angle between the equator plane and the orbit plane)
Ω - right ascension of ascending node (in the equatorial plane the angle between Vernal Equinox direction and the intersection line with the orbit plane in the direction of the ascending arc)
ω - argument of perigee (the angle in the orbit plane at ascending arc from the intersection of the equatorial plane to the closest point of the satellite's orbit towards Earth (the perigee))
ν - true anomaly (depending on time, the angle between perigee and the current satellite position in its orbit)

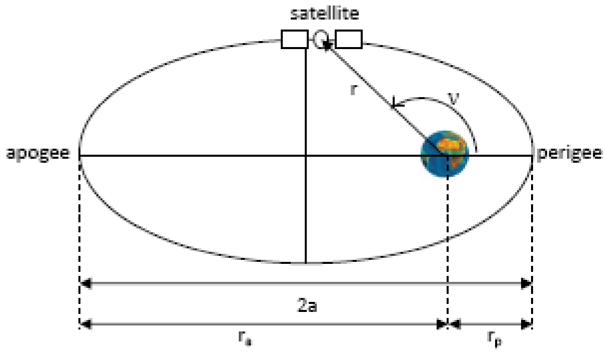

Figure 2: Parameters in the orbit plane.

The Kepler parameters a and ε represent the dimensions and shape of the flight path in the orbit plane, while ν relates to the satellite's current position. Here the radius of closest point of the orbit towards Earth, the perigee $r_p = a\,(1 - \varepsilon)$ and the farest distance, the radius of apogee $r_a = a\,(1 + \varepsilon)$ can be directly derived. The parameter Ω, ω, i determine the orbit plane's position in 3-dimensional space.

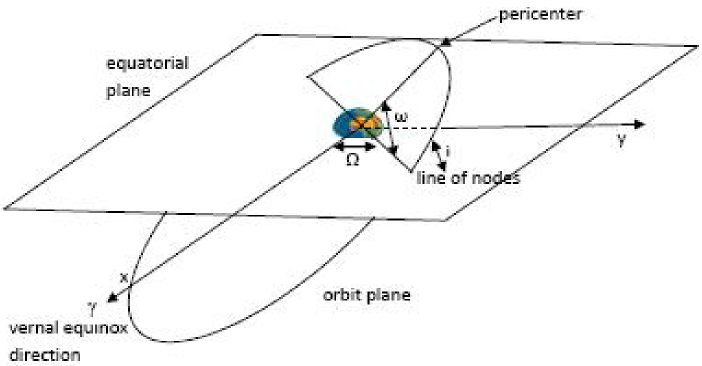

Figure 3: Position of the orbit plane in three dimensions in relation to the equator plane.

The period for one revolution T is only depending on the semi-major axis and the Earth's gravitational constant $\mu = 398\,600.4418\ \mathrm{km^3 s^{-2}}$

$$T = 2\pi\sqrt{\frac{a^3}{\mu}}\ .$$

Several perturbation effects act on such an idealized Kepler orbit: A major effect relates to the inhomogenities of the Earth's gravitational field. In particular the Earth's oblateness (the equatorial bulge) generates a torque rotating the orbit (for i < 90° in westerly direction with negative ΔΩ) at a nodal regression of

$$\Delta\Omega = -\frac{3\pi J_2 R_E^2}{a^2(1-\varepsilon^2)^2}\cos i \qquad [\text{radians/revolution}] = [\text{rad/rev}]$$

and a rotation in the argument of perigee

$$\Delta\omega = \frac{3\pi J_2 R_E^2}{2a^2(1-\varepsilon^2)^2}(4 - 5\sin^2 i) \qquad [\text{radians/revolution}] = [\text{rad/rev}]$$

with the parameters

R_E - radius at Earth equator (6378 km),
J_2 - first tesseral term of the power series expansion of Earth's gravity potential field.
$J_2 = 0.00108263$

2.1 Earth Synchronous Orbits

To describe now the relative motion of a satellite with respect to the Earth's surface, which is essential for observation tasks the following basic definitions are introduced:

A ***subsatellite point*** is defined as intersection of the line between satellite and Earth centre with the Earth's surface. The set of subsatellite points generated during an orbit are called *ground track*.

In order to compare the temporal evolution of observation data, the satellite should observe again after a given period of time the same locations on the surface of the Earth:

An orbit is called ***Earth synchronous***, if after a specific period of time the satellite ground track repeats.

To calculate properties of an Earth synchronous orbit, the effects related to the rotation of the Earth around its axis and the movement of the satellite's orbit plane due to perturbation effects are to be analyzed. In the context of this introductory paper as a first approximation we just consider the J_2-effects of the gravity field, which is the most significant contribution. For a satellite with an orbital period T, the offset between subsatellite points at subsequent equator crossings depends on the Earth's rotation rate (in eastward direction), the so called ***sidereal rotation period*** or ***sidereal day***.

From astronomical observations is known that τ_E is slightly varying with time

$$\tau_E = 86164.10555 + 0.015\ C \quad [s]$$

where C represents the centuries since the year 2000.

As the Earth rotates in eastward direction, the satellite is thus moving relative to the surface in westward direction by an angle

$$\Delta\Phi_r = \frac{T}{\tau_E}\ 2\pi \qquad [rad/rev]$$

As second effect influencing the shift of the subsatellite point at the equator is due to the rotation of the satellite's orbit plane. According to the J_2-model of the gravity potential field

$$\Delta\Omega = -\frac{3\pi J_2 R_E^2}{a^2(1-\varepsilon^2)^2}\cos i \qquad [rad/rev]$$

As $\Delta\Omega$ is positive in eastward direction, these two effects are combined to the total angular shift $\Delta\Phi$ at subsequent equator passages

$$\Delta\Phi = \Delta\Phi_r - \Delta\Omega \qquad [rad/rev]$$

We assumed that an Earth synchronous orbit repeats. Thus after n orbits (n being an integer number), the accumulated shifts by $\Delta\Phi$ in each revolution must be a multiple of 2π.

An Earth synchronous orbit has the property, that integers n (number of orbits until the ground track repeats) and m (number of Earth revolutions until the ground track repeats) exist, such that

$$n \; \Delta\Phi \; = \; m \; 2\pi$$

2.2 Sun and Earth Synchronous Orbits

Comparison of images taken at the same location also would require similar light incidence conditions. Due to the Earth's motion around the Sun, this will in general change in the course of the year. One revolution of the Earth around Sun requires a duration $\tau_S = 3.155815 \cdot 10^7$ seconds, a sidereal year. For a sun synchronous orbit, nevertheless the angle between the sun direction and the orbit plane should remain constant. Thus a nodal regression of the orbit plane (in easterly direction) has to compensate the Earth's motion around the Sun.

The orbit of the Earth around the Sun can as first approximation be assumed as circular (in exact terms the related eccentricity is $\varepsilon = 0.0034$), the sun incidence direction moves by 360° during one year, e.g. by approximately 1° per day). Thus this rotation angle θ of the orbit plane per day is

$$\theta = 2\,\pi \frac{\tau_E}{\tau_S} \qquad \text{[rad/day]}$$

For a satellite orbit with orbital period T the required angular motion is therefore

$$\theta = 2\,\pi \frac{\tau_E}{\tau_S} \frac{T}{\tau_E} \qquad \text{[rad/rev]}$$

With respect to Earth observation tasks, it would be desirable to observe with progressing time the same surface point at identical light incidence. Thus the property, that an orbit is Earth synchronous as well as Sun synchronous, is represented by the constraint

$$\Delta\Omega \; = \; \theta$$

Inserting this into the equation for Earth synchronous orbits, there results

$$n\,(\Delta\Phi_r \; - \; \Delta\Omega) = n\,\left(\frac{T}{\tau_E}\;2\,\pi \; - \; \theta\right) \; = \; n\,\left(\frac{T}{\tau_E}\;2\,\pi \; - \; 2\,\pi \frac{\tau_E}{\tau_S}\frac{T}{\tau_E}\right) \; = \; m \;\; 2\pi$$

This last equality can be converted to the constraint on the orbit period T for an Earth and Sun synchronous orbit

$$T\,\left(\frac{1}{\tau_E} \; - \; \frac{1}{\tau_S}\right) \; = \; \frac{m}{n}$$

The angular shift between two subsequent orbits is

$$\Delta\Phi = \Delta\Phi_r \; - \; \Delta\Omega = \;\; 2\,\pi \;\; T\,\left(\frac{1}{\tau_E} \; - \; \frac{1}{\tau_S}\right) \qquad \text{[rad/rev]}$$

The worst case distance between two successive orbits occurs at the equator. At the Earth radius at equator $R_E = 6378$ km this implies to a distance of $\Delta\Phi \cdot R_E$ between subsequent ground tracks. In the following chapter this will be further expanded taking into account observation parameters like swath width to analyze ground coverage of the areas observable from the satellite.

2.3 Ground Coverage

The surface area observable from the spacecraft is limited by the tangential line to the Earth's surface. Thus from the spacecraft at an altitude h above surface the visible horizon is characterized by the angle ρ and by the angle λ_0 from Earth centre's perspective (cf. Figure 4).

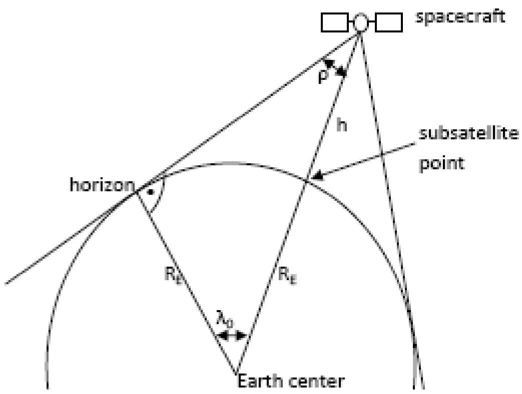

Figure 4: Observable surface area from the satellite.

Assuming a spherical Earth, the line from the spacecraft to the horizon is perpendicular to the Earth's radius, thus the following relationships hold in the triangle formed between spacecraft, Earth centre and horizon with the hypothenusa R_E+h

$$\rho + \lambda_0 = 90°$$

$$R_E = (R_E + h) \cos \lambda_0 = (R_E + h) \sin \rho$$

A specific target point with known longitude Λ_t and latitude Θ_t in this visibility range is observed from a known orbit position of the satellite, leading for the related subsatellite point to a longitude Λ_s and latitude Θ_s . Then the characteristic parameters are the *nadir angle* η at the satellite (the angle Earth centre/spacecraft/ target) and the *Earth central angle* λ (the angle spacecraft/Earth centre/target), as well as the *spacecraft elevation angle* ε from the local horizon at the target towards the satellite.

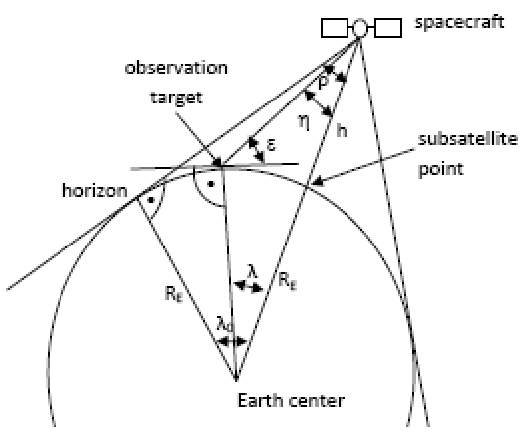

Figure 5: Observation of target points in the satellite's field of view.

The angular distance λ between subsatellite and target point at the Earth's surface can be determined from spherical geometry (for $\lambda < 180°$) as

$$\cos\lambda = \sin\Theta_s\ \sin\Theta_t + \cos\Theta_s\ \cos\Theta_t \cos|\Lambda_s - \Lambda_t|$$

From λ the nadir angle η can be calculated

$$\tan\eta = \frac{\frac{R_E}{h+R_E}\sin\lambda}{1-\frac{R_E}{h+R_E}\cos\lambda}$$

Finally the spacecraft elevation angle can be either derived from

$$\lambda + \eta + \varepsilon = 90°$$

or from $$\cos\varepsilon = \sin\eta/(R_E/(h+R_E))$$

For a specific instrument onboard the spacecraft a field-of-view (FOV) or a footprint area refers to the area it observes at a specific point in time. So the beam width of an instrument allows to see target points corresponding to a related variation range of nadir angles η (when taking the satellite's perspective) or Earth central angles λ (taking the Earth's perspective). Define λ_{max} as *maximum Earth central angle* achievable by selecting appropriate instrument pointing and spacecraft attitude. Then for each point in time a circle on the Earth surface around the current subsatellite point with radius related to λ_{max} determines the access area for observations. Thus a *swath width* of $2\lambda_{max}$ (an angular deviation of λ_{max} on both sides perpendicular to the ground track) characterizes the surface coverage for the spacecraft. The time in view T_{view} of a specific surface point P crucially depends on off-track angle λ (the angle between P and its perpendicular projection to the ground track; necessarily is $\lambda < \lambda_{max}$). For a circular orbit with period T the time in view is

$$T_{view} = \frac{T}{180°}\cos^{-1}\left(\frac{\cos\lambda_{max}}{\cos\lambda}\right)$$

where $2\cos^{-1}\left(\frac{\cos\lambda_{max}}{\cos\lambda}\right)$ is the range for the true anomaly at which P can be kept in the field of view. Related properties for distributed multiple satellites with respect to temporal and spatial resolution will be further analyzed in chapter 3. In the following section this theory will be applied first to characterize contact periods to ground stations, being a crucial mission design parameter.

2.4 Ground Station Contact Period Analysis

Orbit selection is driven by observation objectives, but also by operational and satellite design constraints. The maximum periods between contacts to ground control stations have an implication in sizing the data storage system on-board to provide sufficient capacity to accommodate all observation data until the next downlink occurs. Duration of these ground contacts affect the needed transmission capacities to transfer all acquired data. With respect to mission operations on-board autonomy requirements are driven by the periods between ground contacts. The analysis from section 2.3 is now specialized for surface target points being ground stations. The visibility area from the ground station is a cone with central angle depending on the elevation angle ε. This cone intersects with a ball around the Earth's centre with radius $R_E + h$ at orbit altitude in a circular segment. If the flight path crosses this segment, at entry as well as at exit the parameters λ_{max}, η_{max}, ε_{min} apply, while at the closest approach of the path to the ground station λ_{min}, η_{min}, ε_{max} occur.

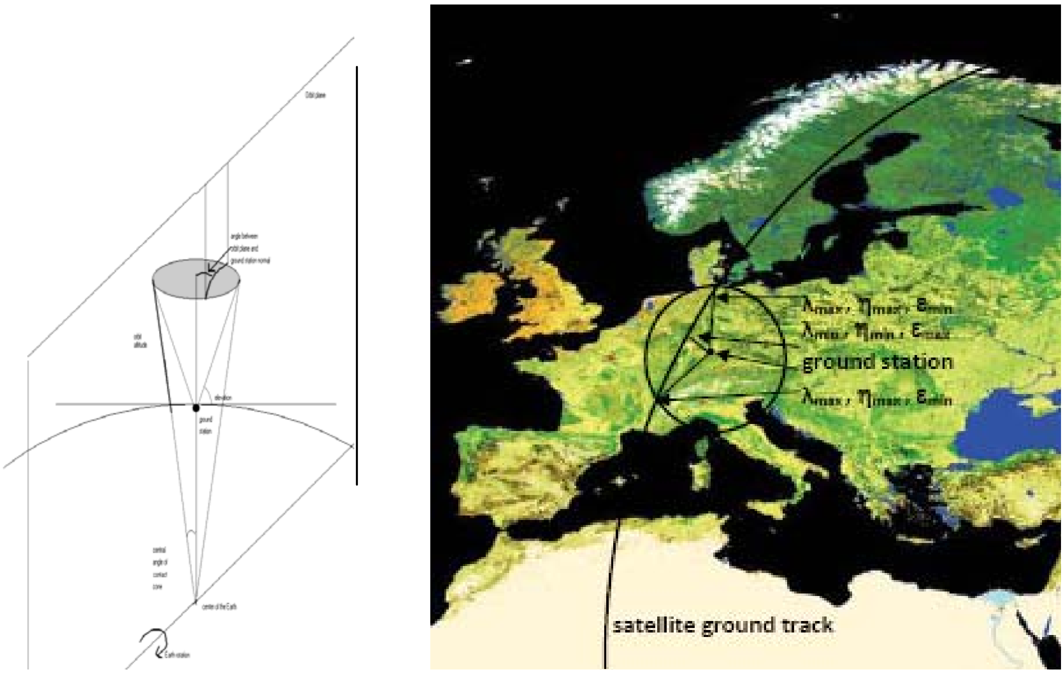

Earth image courtesy of ESA

Figure 6: Contact geometry to the ground station.

According to section 2.3 these angles can be calculated with a known minimum necessary elevation of the ground station ε_{min} to establish contact (depending of the topology of the environment, typically it is about 5°) as

$$\sin \eta_{max} = \cos \varepsilon_{min} \frac{R_E}{h + R_E}$$

$$\lambda_{max} = 90° - \varepsilon_{min} - \eta_{max}$$

This also corresponds to the maximum range D_{max} between ground station and satellite

$$D_{max} = R_E \; \sin \lambda_{max} / \sin (\eta_{max})$$

In order to calculate the crucial time in view T_{view} , in addition to λ_{max} also the minimum Earth central angle λ_{min} at the closest point of the flight path to the ground station is to be determined. Thus, with known longitude Λ_{gs} and latitude Θ_{gs} of the ground station

$$\sin \lambda_{min} = \sin (90° - i) \; \sin \Theta_{gs} \; + \; \cos (90° - i) \; \cos \Theta_{gs} \; \cos (\Lambda_{gs} - \Lambda_{node} + 90°)$$

with Λ_{node} being the longitude of ascending node in the Earth-fixed coordinate system (while Ω is defined in the sidereal coordinate system, Λ_{node} is rotating with the Earth). Thus the total time in view is

$$T_{view} = \frac{T}{180°} \cos^{-1}\left(\frac{\cos \lambda_{max}}{\cos \lambda_{min}} \right)$$

For the optimal case that the satellite passes in the zenith of the ground station there results $\lambda_{min} = 0$ and the maximal contact time results from this equation as

$$T_{view\ max} = T\ \frac{\lambda_{max}}{180°}$$

2.5 Eclipse Periods

Limitations on satellite activities result, when the satellite enters into the zone where the Sun light is occulted by the Earth, the Earth shadowed zone or eclipse period. The angle β between the Earth-Sun vector s and the orbit plane is derived by using the normal vector to the orbit plane n by

$$\sin \beta = s \bullet n$$

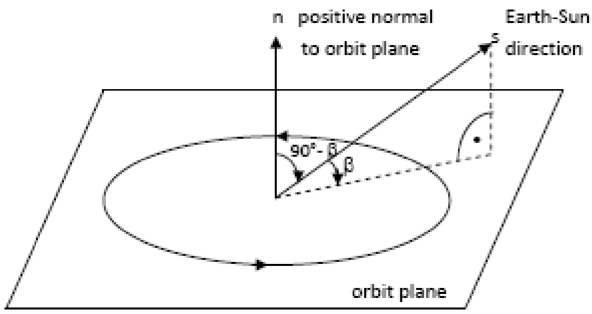

Figure 7: Geometry of the Sun-orbit angle β.

Assuming Earth generates a cylindrical shadow as first approximation, the Earth central angular radius β* at entry into the eclipse is

$$\beta^* = \sin^{-1}\left(\frac{R_E}{h + R_E}\right) \qquad \text{for } 0° \le \beta^* \le 90°$$

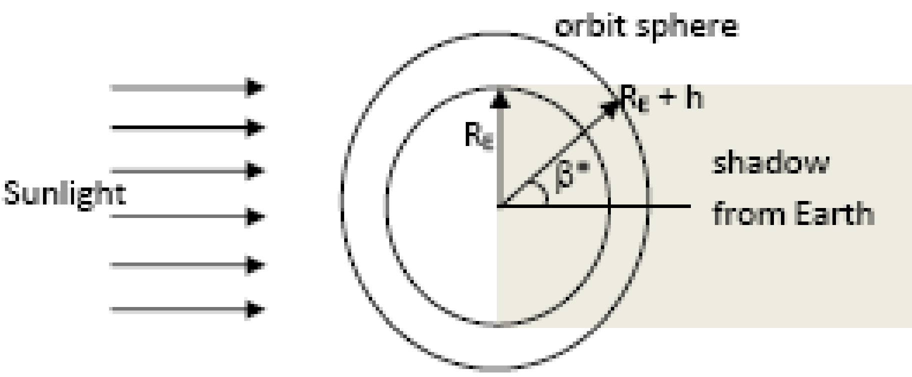

Figure 8: Schematic of eclipse geometry.

The angular arc of the orbit in the shadow cylinder is $2\cos^{-1}$(cos [illegible] /cos( ) , thus the eclipsed fraction of the orbit F_e depending on the Sun-orbit angle β is

$$F_e = ([\cos]^{-1}(-1) (\cos [(^{1} *] /\cos( ))/(180°) = \frac{1}{180°} \cos^{-1}\left(\sqrt{(h^2 + 2R_E h)}/((R_E + h) \cos( )\right)$$

2.6 Exemplary Mission Analysis

In this section for a LEO-mission an analysis to optimize parameters is performed for an orbit at altitude h= 600 km. Inclination i could vary between 0° and 53°. With respect to eclipse periods the annual variation of β in an equatorial orbit is between 0° and 23.44°. The effect on F_e is minimal as displayed in the plot of Figure 9 and Figure 10, thus thermal variations are very limited.

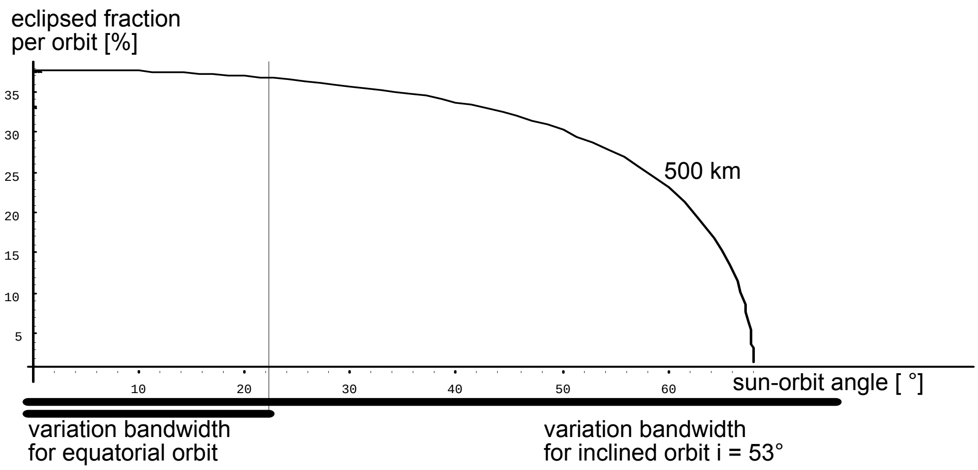

Figure 9: The eclipsed fraction F_e as a function of the sun orbit angle β in an orbit altitude h= 500 km. For an equatorial orbit (i=0°) and an orbit with inclination i=53° the annual variation of sun-orbit-angle β is marked below.

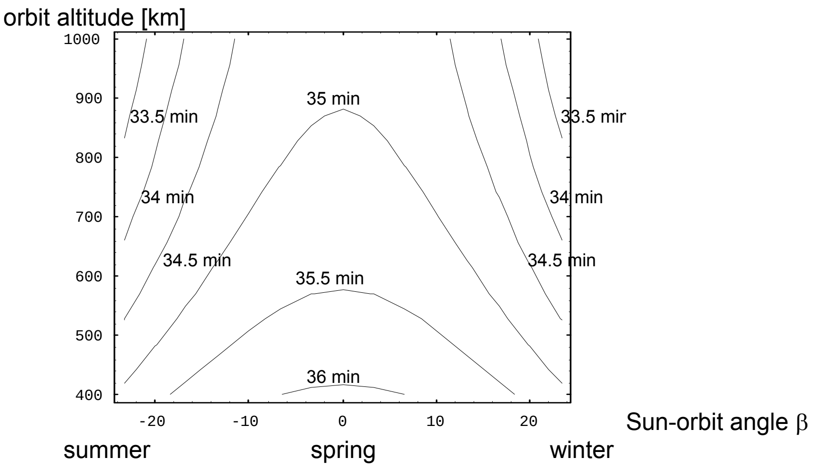

Figure 10: For the equatorial orbit in an altitude range between 400 km and 1000 km the eclipse duration in minutes is represented in relation to seasonal changes of β.

For an orbit inclination of 53° displays a broad variation of β between 0° and 76.44°. Related eclipse periods vary between 0 and 35.4 minutes per orbit, requiring a robust thermal design.

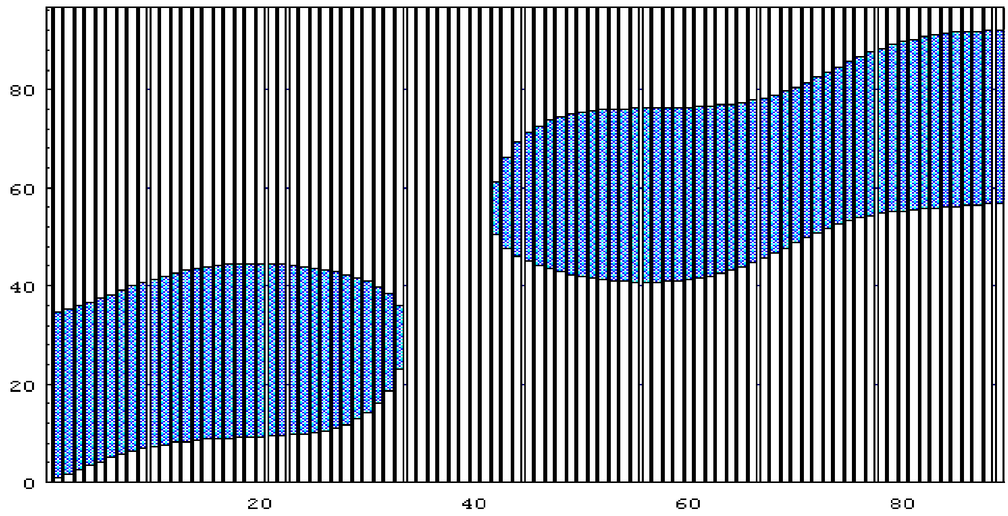

Figure 11: Variation of eclipse periods for 3 months. Each column is a representative orbit with the eclipse duration marked by the dark segment.

The orbit with inclination i=53° and h=600 km displays a drift due to J_2-effects

$$\frac{d}{dt}\Omega = -4.4° \text{ [°/day]}$$

One major advantage of this orbit is that operations can be done from a ground station in Germany. There exist contacts during several subsequent passes, followed by periods without contacts (cf. Figure 12). The periods without link capabilities can be analyzed by using the station-orbit angle (the angle at the Earth's center between the orbit plane and the ground station direction; cf. Figure 6). Figure 13 presents the angular variation for a ground station in southern Germany. Contacts are only possible if the station-orbit angle is smaller than the central angle of the contact cone (the cone originating in the Earth centre covering the same segment of the sphere at orbit altitude as the ground station). With a minimum necessary elevation angle of 5° of the ground station, this leads for the nominal orbit to a central angle of the cone of 19.42°. As displayed in Figure 13, there results a contact potential for 43.5% of a day, leading on average to six ground contacts per day, each extending up to 10.4 min.

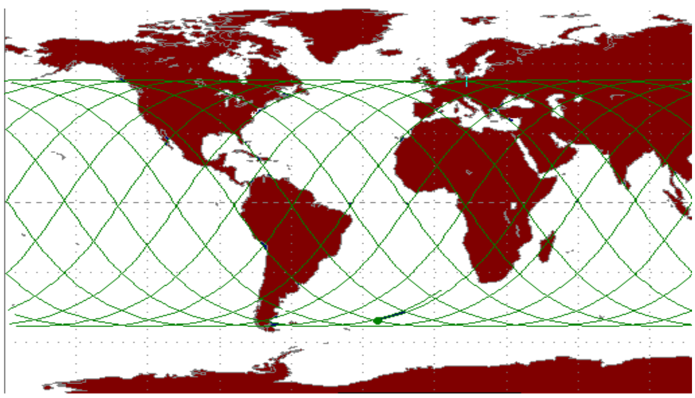

Figure 12: Ground track generated by the orbit with 53° inclination in altitude h=600 km.

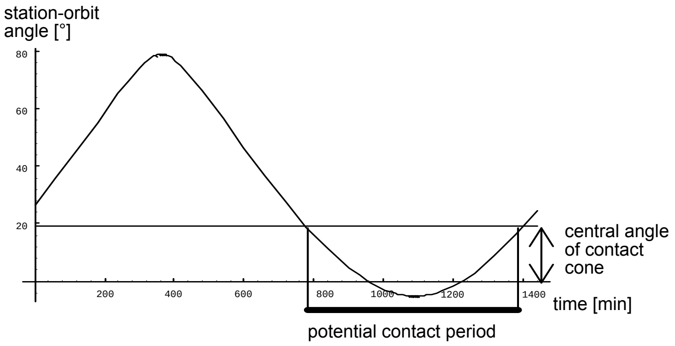

Figure 13: Diurnal variation of the station orbit angle, specifying the window for ground station contacts.

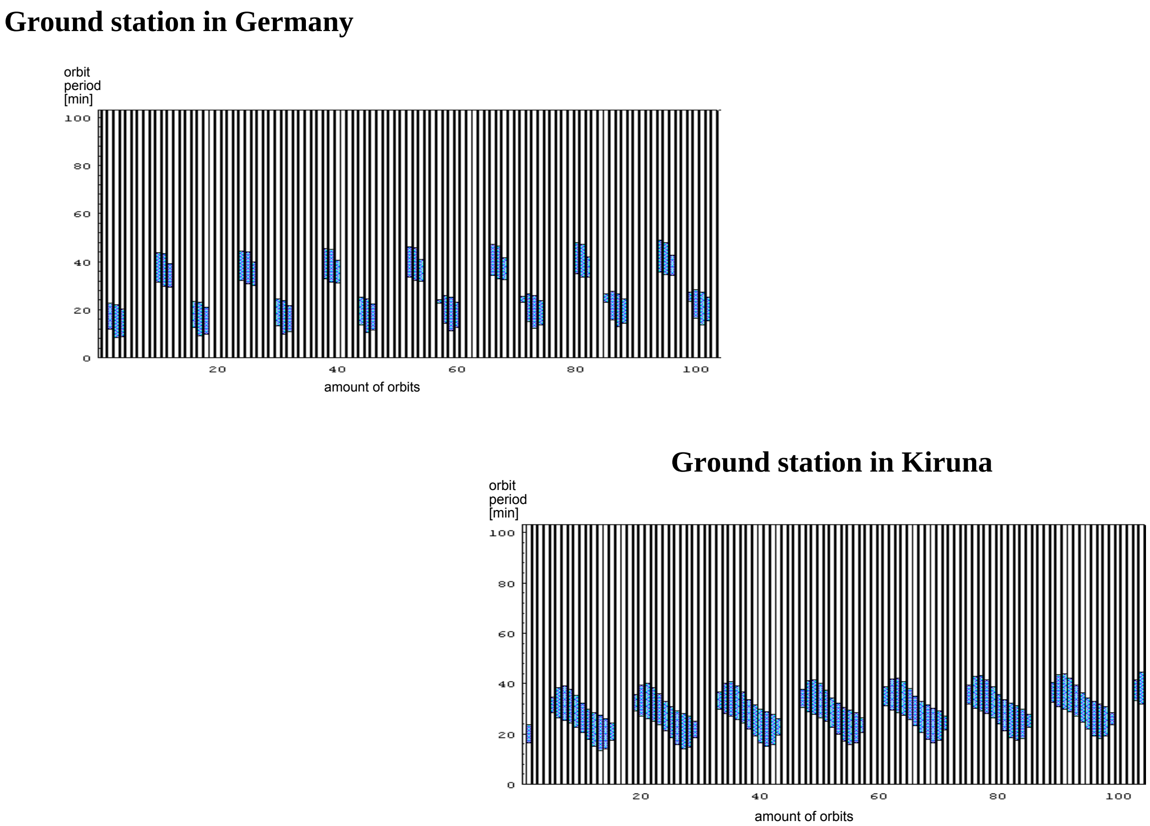

Figure 14: Typical sequence of contact periods (dark segments) for a Sun-synchronous orbit in 900 km altitude (i= 98°) related to a ground station in Germany (above) and one near the north pole in Kiruna (below).

Thus, particular advantages of the inclined orbit (i = 53°) compared to the equatorial orbit are that:

- the ground station can be located in Germany,
- the solar arrays generate more power during mission lifetime, as the eclipsed periods are shorter,

while the disadvantages inc1ude:

- periods between 13.75 and 15.75 hours without ground contact,

- thermal control is more demanding, as eclipsed periods vary very much,
- magnetometers of the attitude control system suffer from more frequent disturbances near the poles in the Earth's magnetic field,
- the radiation noise is larger, as the orbit crosses the south atlantic anomaly and approaches closer to the poles.

3.0 SATELLITE CONSTELLATION AND FORMATION CHARACTERISTICS

Nominal orbits for the different satellites are to be selected, such that their combination achieves the application objectives with respect to spatial and temporal resolution at a minimum amount of satellites. The transfer of satellites into these target orbits and the efficient deployment of satellites are to be analyzed. After having been arrived in the target orbits an appropriate formation has to be maintained and the control activities for station keeping are to be provided.

Another interesting application could be the creation of 3-dimensional pictures out of data collected by a swarm of satellites, doing observations of the same area at different viewing angles. Examples were the tandem missions of traditional satellites like ERS-1 and ERS-2, Landsat 7 and EO-1. Taking advantage of being able to place several small satellites into one launcher it would be possible to establish efficiently such formations or constellations for Earth observation.

3.1 Formation Flying Architectures

In order to perform complex tasks in a broad range of applications formations of vehicles with varying dynamics, such as groups of aircrafts, UAVs, submarines and land vehicles are analyzed. In general three different architectural approaches are discussed:

- ***Virtual Structures***: the entire formation is treated as one single structure controlled by a centralized planner. The dynamics of the complete structure is translated into a desired motion for each vehicle, which has an individual tracking control.
- ***Behavioral strategies***: in this distributed control approach following inspirations from nature (flock of birds, school of fish), several desired behaviors for each agent (e.g. move-to-goal, avoid-collisions, avoid-obstacles, maintain-formation, etc.) are specified. The control action of each agent is the weighted average of the controls for each behavior.
- ***Leader-follower***: vehicles are divided into leader(s) and followers, the followers track position and orientation of a designated reference point (leader) with a prescribed offset. It can be implemented as
  - *Absolute control architecture*, where a central controller sends position and velocity commands to each vehicle regulating its own position, or as
  - *Relative control architecture* sending absolute position and velocity commands of the leader, while the followers regulate their own position relative to the leader.

  While there is a transparent group behavior, the leader is a particularly sensitive position.

As discussed before for single spacecrafts, idealized Keplerian orbits are subject to perturbation effects from mass inhomogeneties of the Earth's gravitational field, atmospheric drag, solar radiation pressure, third body perturbations (e.g. Moon, Sun). For spacecraft in close-by orbits the dynamics of the relative motion is described by the Euler-Hill-Clohessy-Wiltshire equations [see Sidi, 2001; Vallado, 1997].

3.2 Coverage by a Constellation

Constellations of LEO-satellites are introduced to benefit from the shorter distance to the Earth's surface, in particular from shorter signal propagation periods, lower energy intensity and power needs for data transmission and instrumentation. On the other side the high relative velocities relative to the surface imply short contact periods to ground stations or short observation periods of specific surface areas. Therefore several satellites in appropriate complementary orbits are placed to increase coverage. When placing the satellites in similar orbits (with respect to altitude, eccentricity, and inclination) perturbations affect all satellites in a similar way and station keeping manoeuvres to keep the satellite topology can be limited with positive implications for the satellites' lifetimes. A frequently used class is the Walker Delta pattern constellation [Walker, 1984], with the objective of provision of a continuous coverage of the Earth's surface by a minimum number of spacecraft. Despite this being a frequent aim, for different objectives alternative constellation patterns might be more appropriate. Typical non-Walker constellations address planes perpendicular to each other (by example a combination of a polar plane with an equatorial plane). For a Walker constellation with inclination i, total number of satellites t, number of equally spaced orbit planes p with t/p equally spaced satellites in each plane, and the relative phase difference between satellites in adjacent planes f ($0 \le f \le p-1$, measured in the direction of motion from the ascending node to the closest satellite in units of 360°/t), the standard notation for a constellation is presented in the following form:

$$i: t/p/f$$

The Gallileo navigation satellites are by example placed as a 56°: 27/3/1 constellation, having 27 satellites in orbit, inserted in 3 orbit planes separated by $\Delta\Omega = 120°$. Each of the 3 orbit planes with an inclination i = 56° hosts 9 satellites at angular distances of 40°. The phase shift between adjacent orbits is $f \bullet 40°/3 = 1 \bullet 13\frac{1}{3}° = 13\frac{1}{3}°$.

Let $s = t/p$ satellites be equally spaced at an angular distance $\Delta\nu = 360°/s$ in a orbit plane. If in comparison to $\Delta\nu$ the maximum Earth central angle λ_{max}, as discussed in section 2.3, is

- $\Delta\nu < 2\,\lambda_{max}$, there is an area of continuous coverage, often called *street of coverage* (cf. Figure 15) with an angular range of λ_{street} on both sides of the ground track,
- $\Delta\nu > 2\,\lambda_{max}$, the coverage will be interrupted along the swath.

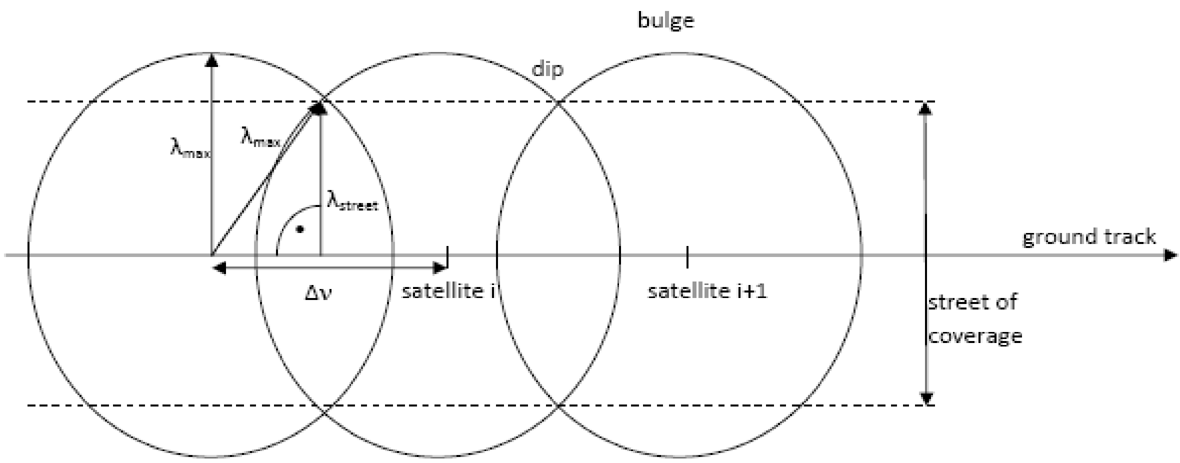

Figure 15: Topology of satellites in the same orbit plane.

The width of the *street of coverage* λ_{street} can be calculated from

$$\cos \lambda_{street} = \cos [\lambda_{max}] /(\cos\ \Delta(/2)$$

Adjacent orbits planes can now suitably be coordinated such that the bulges of the one orbit plane fill in to the dips of the other plane (cf. Figure 16). So for guaranteeing a continuous coverage the maximum distance between adjacent orbit planes D_{max} can be selected as

$$D_{max} = \lambda_{street} + \lambda_{max}$$

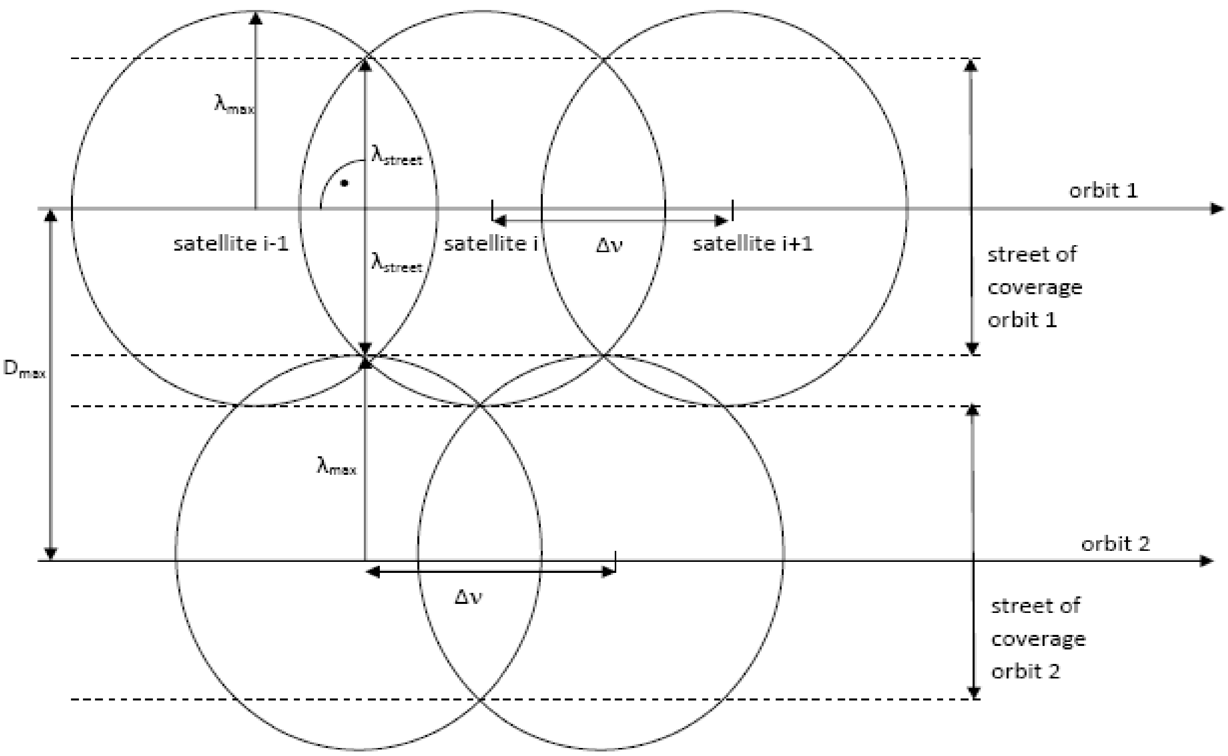

Figure 16: Suitable coordination patterns to be achieved for two adjacent orbits, moving in the same direction, by the choice of f = Δν/2.

This effect just applies if the satellites are synchronized with similar velocity vectors. It should just illustrate that combinations of the different orbit parameters complicate optimisation for analysing coverage in distributed multi-satellite systems. Procedures for the replacement of defect satellites in a constellation need to be considered at deployment. Very often also soft parameters, like the flexibility with respect to growth potential for the satellite constellation are crucial.

3.4 System Requirements for Remote Observation by Distributed Small Satellites

For coordinated observations by swarms of small satellites, challenging technical research problems are to be solved. A necessary requirement is the ability of the satellites to maintain the formation. Thus the position and attitude relative to each other is to be determined with appropriate accuracy, before control actions correct towards the target position in the formation. All satellites of the swarm have to be equipped with suitable sensors and actuators to perform such manoeuvres. Especially for pico- and nano-satellites there is still a need for small, low weight sensors and actuators. Within current technology it is by example not possible to integrate a star tracker at pico-satellit level, nevertheless an high accuracy attitude determination is desired. Recent activities in the field of sensor development demonstrate implementation of extremely small components by MEMS technology.

The UWE-2 satellite employs a GPS system for position determination and subsequent orbit determination. The companion pico-satellite BEESAT from TU Berlin carries a 3-axis attitude control system by three reaction wheels [cf. Schilling, Brieß, 2008]. The University of Toronto will demonstrate by the CanX-2 satellite at nano-satellite level actuators for formation control by using thrusters and 3-axis-stabilized attitude control. The motivation for this mission is the test of enabling technology for formation flying. In the next step the Can-X4 and Can-X5 satellites are planned for an autonomous formation flight. Thus, future missions will perform complex formation manoeuvres with pico- and nano-satellites, but there is still significant research necessary in order to establish appropriate attitude control and formation control systems for satellites in the pico- and nano-satellite class.

4.0 COMMUNICATION IN LOW-EARTH-ORBIT SATELLITE SWARMS

The communication and tele-operation infrastructure provides a key element in establishing distributed satellite systems: formation flying information related to the status of each satellite is to be exchanged and observation data are to be transferred. The amount of data to be exchanged increases with the size of the satellite swarm. Thus efficient implementation of data pre-processing procedures, as well as intersatellite links and links to ground stations are to be analyzed. Here adaptations of terrestrial technologies for mobile distributed systems to the space environment are of particular interest.

4.1 IP Infrastructure for Spacecraft Applications

In distributed applications on Earth the internet protocols TCP/IP became the established standard and attracts significant development efforts for further improvements. To benefit from these terrestrial activities, transfer of these technologies to the space environment is investigated, in particular adaptations to significant delays and at higher noise levels are to be analyzed. First experiments related to IP in space were performed 1999 by NASA at the UoSat-12 mission. One of the first missions, totally operated only over the TCP/IP protocol stack, was the CHIPsat mission launched in 2003 from NASA and the Space Science Laboratory in Berkley.

In 2005 the pico-satellite UWE-1 (University Würzburg's Experimental satellite) was launched with the main scientific objective to optimize Internet Protocol parameters in adaptation to the measured space environment [Schilling, 2006]. UWE-1 had a mass below 1 kg, followed the CubeSat standards [Twiggs, 2002] and carried the on-board data handling system µ-Linux, implemented on a microcontroller. Thus advantage could be taken from integrated, appropriate IP-stack for related telecommunication experiments. The advantages of IP and its higher layer protocols (e.g. TCP, UDP) are the world wide usage, resulting in a fully tested reliable protocol stack and a broad spectrum of available applications using the IP interface. UWE-1 communication was based on a commercial transceiver, normally used by radio amateurs for data transmission via packet radio. The main experiments were related to cross layer optimizations between AX.25 and higher protocol layers (i.e. IP) and to application layer protocols like HTTP and TFTP.

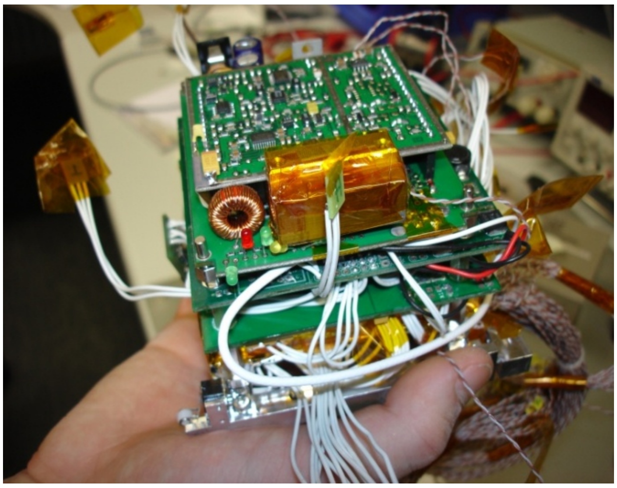

Figure 17: The UWE-2 boards display highly integrated pico-satellite electronics. Here from top to bottom the following boards can be seen: telecommunication (UHF / VHF), power distribution, data processing (H8, µLinux), GPS receiver.

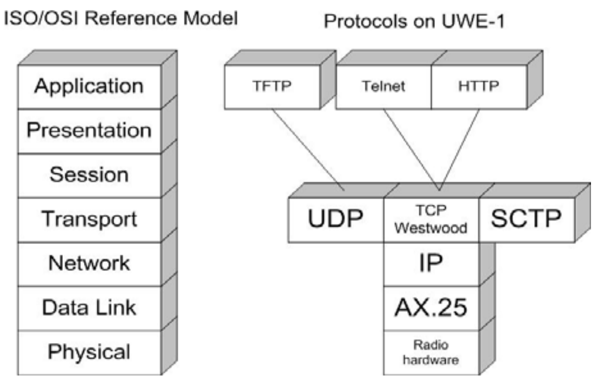

Figure 18: the specific implementation of ISO/OSI reference model layers on-board of UWE-1. Here for comparison reasons several transport layer alternatives were realized.

A major disadvantage of the TCP/IP protocol stack is the performance problem of the TCP protocol in space conditions. As the TCP protocol was intended for usage in the terrestrial internet, a congestion avoidance algorithm decreases the transmission rate, if congestion occurs. This behavior is an essential feature of TCP in the terrestrial internet, when the network is overloaded by traffic. A congestion situation in the terrestrial internet is indicated by the loss of data packets. In a satellite communication the situation is totally different, loss of packets are normally caused by transmission errors, nevertheless TCP reacts in this situation with decreasing the transmission rate. Therefore it is important to choose very carefully the communication protocols. An alternative is the usage of UDP instead of TCP, a connectionless transport protocol. In this case the application layer has to provide mechanisms to guarantee the correct reception of data packets. Another possibility is to use a TCP extension protocol, which overcomes typical problems of TCP.

The results of the UWE-1 experiments displayed, that it is possible to use IP on a CubeSat for communication, but different optimizations are necessary to enable a reasonable telecommunication between satellite and ground stations. Especially the high Packet Error Rate (PER) observed on the communication link with UWE-1 has influence on the performance of the AX.25 protocol. The measured PER values are presented in figure 19. The values are expressed in terms of confidence intervals, the variance of these intervals reveal the necessity to improve the combination between AX.25 and IP with additional redundancy for the communication link. Further redundancy for the telecommunication can be generated by hardware or software algorithms to solve the problems of high error rates.

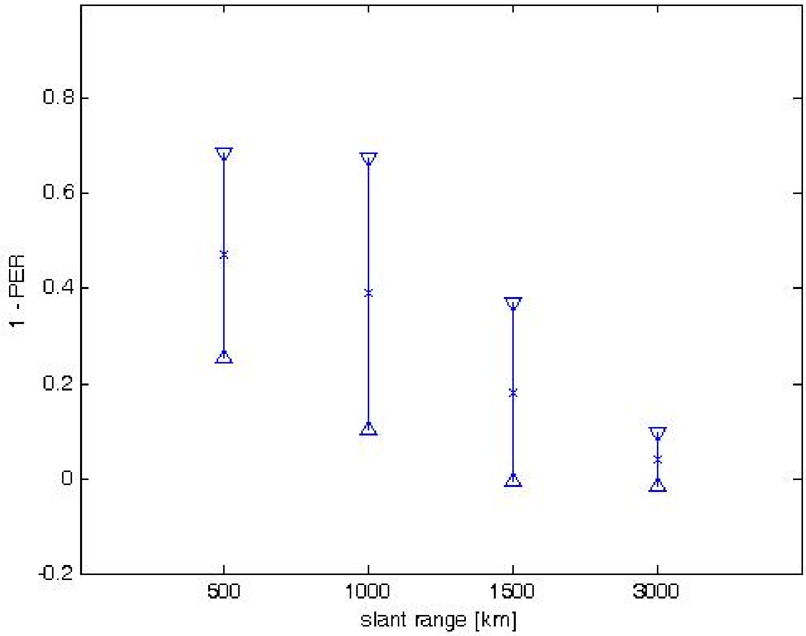

Figure 19: PER determination for the AX.25 radio link.

4.2 Ground Station Networks for Satellite Swarms

The intensive activities in development of small satellites initiated the establishment of many ground stations in academia all over the world. Due to the limited bandwidth of small satellites, it is here especially desirable to increase the contact periods by using multiple interconnected ground stations for data transmission. Thus, a consistent homogeneous telecommunication framework for space and ground segment based on Internet Protocols promises interesting capacities for teleoperation of these small satellites.

Current activities to implement such ground station networks are the “Global Education Network for Satellite Operation (GENSO)”, the “Ground Station Network (GSN)” of the Japanese UNISEC group and the “Mercury Ground Station Network” initiated by Stanford University.

The UWE-1 ground station (c.f. Fig.20) was set up on the University Würzburg campus with capabilities to communicate with satellites in the 2m and 70 cm frequency bands.

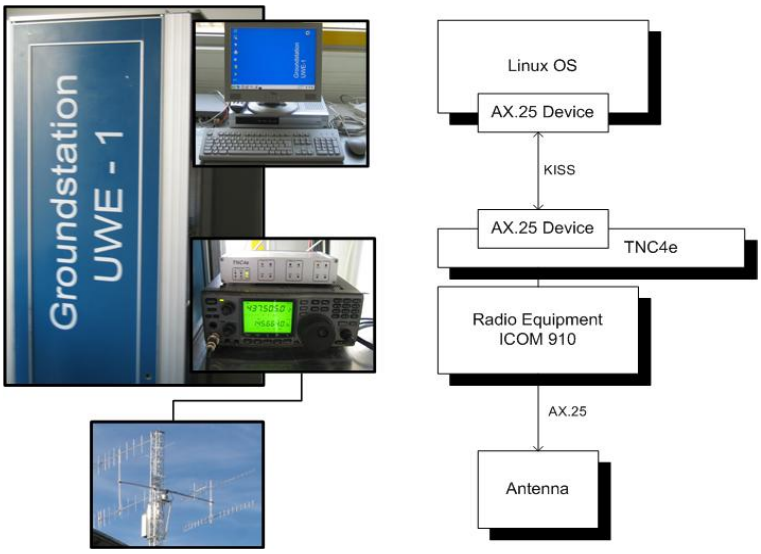

Figure 20: Realisation of the UWE ground station.

A critical point for ground station networks are cross layer dependencies between IP and lower protocol layers, like AX.25 as in case of UWE-1. It is only relevant when a direct connection between the satellite and the remote controller over IP is used. The AX.25 protocol is a data link layer protocol designed for amateur radio networks. The AX.25 protocol can be operated in a connection oriented (virtual circuit) mode or in a connection less (datagram) mode. Connection oriented communication is already provided by transport layer protocols like TCP thus conflicts with this second acknowledgement system could arise, if insufficient coordination with higher layers is established. Thus, the parameterization of the Medium Access Control (MAC) is to be implemented, for avoiding collisions between sending stations by delaying of sending attempts.

4.3 Mobile Ad-Hoc Networks in Space

Establishment of robust network communications attracts significant research efforts in terrestrial applications. A mobile ad-hoc networks (MANet) combines several stations to a self-organizing telecommunication network with integrated initialisation and reconfiguration capabilities, in particular in case of deffects or of changes in the topology. Therefore in formations of satellites, exhibiting high dynamics and link interruptions, a reconfiguration of the communication path via several members of the space and ground segment promise significant increses in robustness. Related routing methods are therefore to be analyzed.

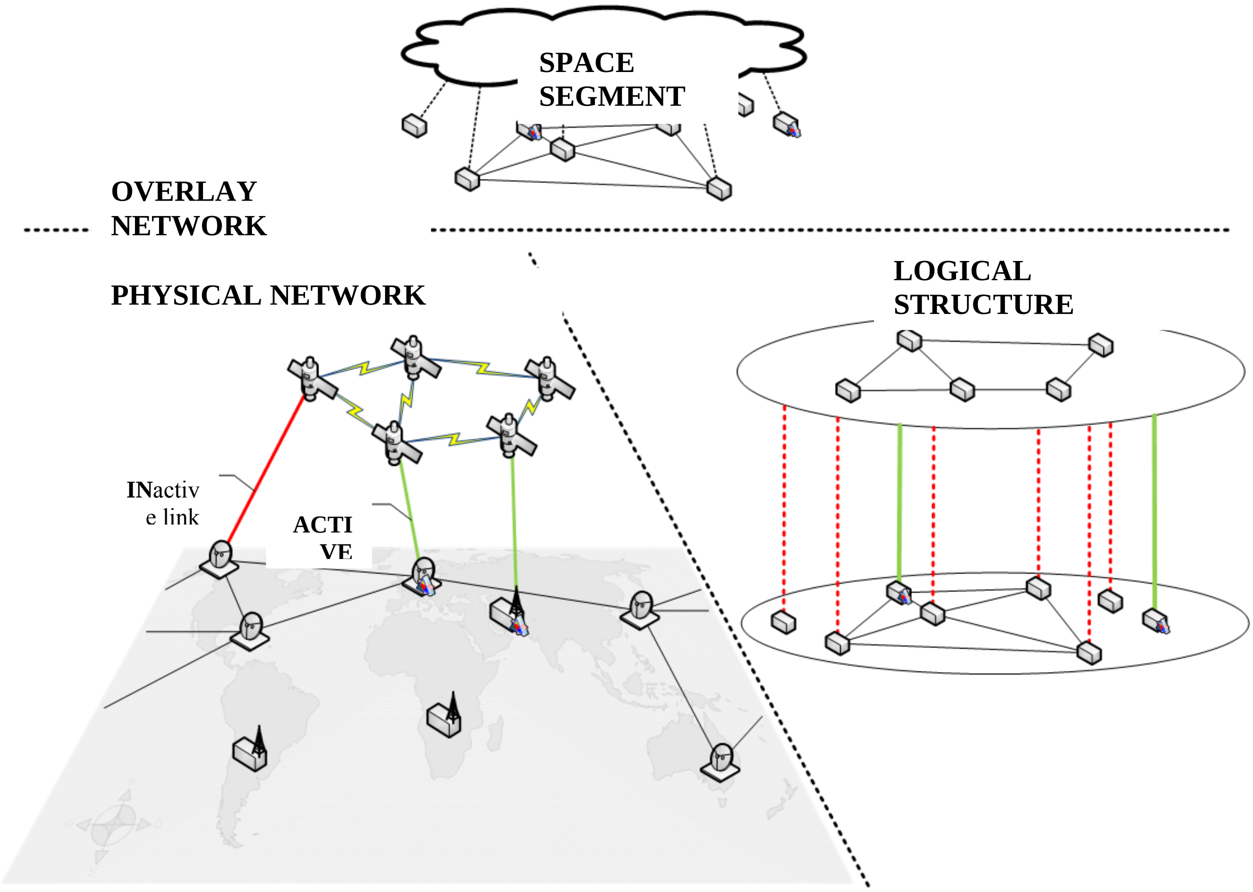

Figure 21: Schematic of an overlay Network approaches for an integrated space and ground segment taking into account the available physical network structure and the abstracted logical structure.

At the University Würzburg a MANet demonstrator and test facility based on WLAN (IEEE 802.11) has been installed, consisting of a system of several mobile robots and fixed stations as nodes (cf. Figure 22).

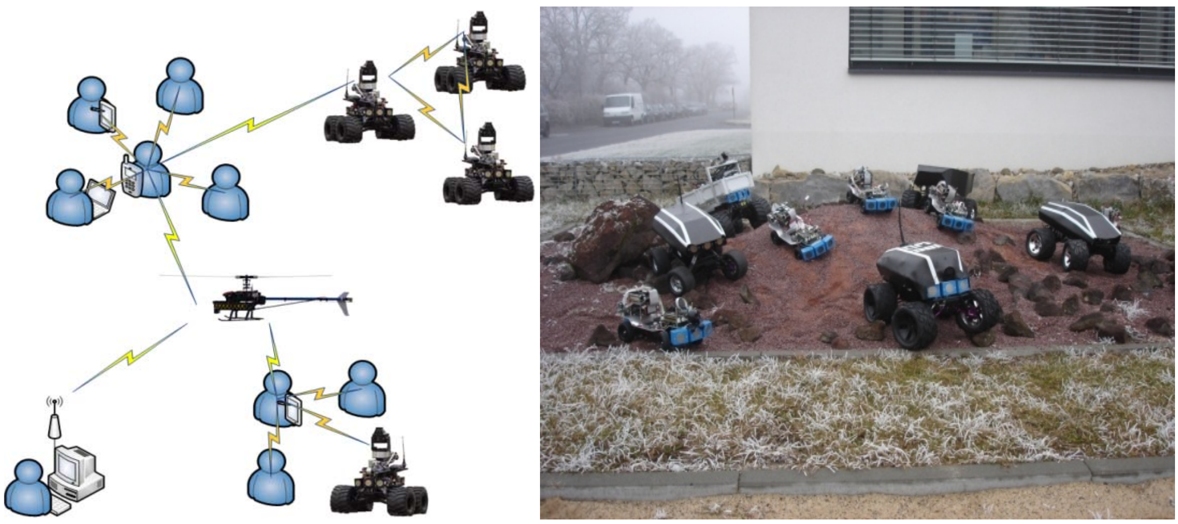

Figure 22: Network of mobile systems with heterogeneous dynamics.

In this test facility experiments to prepare future MANet applications in space have been performed with respect to re-routing performance. Typical ad-hoc routing protocols developed for mobile systems were compared in teleoperation scenarios for mobile robots, including:

- Reactive protocols, such as "Ad-Hoc On-demand Distance Vector (AODV)" or "Dynamic Source Routing (DSR)",
- Proactive protocols, such as "Optimized Link State Routing (OLSR)",
- Hybrid protocols, such as "Better approach to mobile ad-hoc networking (BATMAN)".

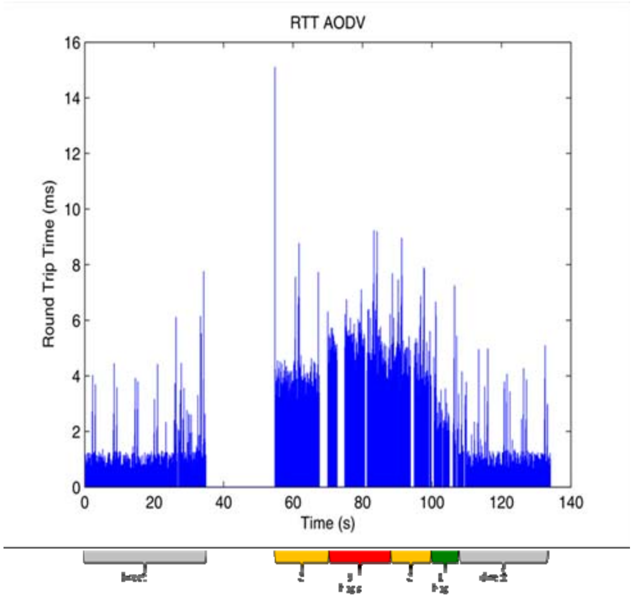

Figure 23: Typical round trip time behaviors for a changing transmission topology, displaying in particular the significant transmission interrupts due to route reestablishment.

A software system has been developed to record during test runs the crucial data about neighbors, route requests, potential routers, link costs and hop counts. Thus resulting characteristics of the packet stream like packet loss rates, time needed for route reestablishment, packet inter-arrival time, network topology and bandwidth can be evaluated. Files from the different nodes are to be synchronized (with respect to time or to events). Typically default parameter settings need to be adapted to the specific scenario to exhibit reasonable performance.

Table 1: Performance comparison for test runs with tuned parameter settings in the protocols.

Protocol	Packet Loss	min. Time for Rerouting	max. Time for Rerouting
OLSR	32.6%	5.0 s	< 21.6 s
DSR	28.8%	2.0 s	< 40.4 s
BATMAN	16.0%	0.8 s	< 26.2 s

The performance measurements turned out to be very sensitive to noise effects, thus a careful setup is necessary to generate comparable results. In preparation of establishing MANets in space also adaptation procedures of protocols to the specifics of the encountered space environment are to be investigated.

5.0 CONCLUSIONS

The paradigm shift from large spacecrafts incorporating multiple payload capabilities to decentralized, distributed small satellite systems raises interesting research topics. Particular advantages in the context of Earth observation and surveillance are higher fault tolerance and robustness of the overall system. Such systems are scalable in a sense that according to application needs additional satellites can be added in order to increase resolution and coverage. The current progress in gun launches (with railguns or light gas guns) to orbit promise interesting quick future reaction capabilities for very small satellites (with a mass of some kg). Nevertheless high resolution data and high bandwidth links can only be provided by traditional large satellites. Thus combinations of coordinated satellite systems composed of few large and many small satellites might complement each other in order to provide the required data quality as well as flexibility and robustness.

Swarms of small satellites offer in particular for Earth observation applications interesting innovative approaches. Satellites in Low Earth Orbit (LEO) enable high spatial resolution on ground and offer interesting potential for applications like disaster monitoring. Due to the low orbit, these satellites exhibit a high relative velocity to reference points on ground, resulting in short observation and communication contact periods in the target areas. One approach to that problem is a higher temporal resolution by satellite constellations with several satellites in the same orbit. The achievable temporal and spatial resolution of such a formation opens new application areas in bio-monitoring and surveillance.

ACKNOWLEDGEMENTS

The support of DLR and ESA for the UWE-projects as well as the enthusiastic contributions of my collaborators Marco Schmidt, Florian Zeiger, Stephan Busch and Rajesh Shankar are acknowledged and formed the basis for this contribution.

REFERENCES

Alfriend, K. T., S. R. Vadali, P. Gurfil, J. P. How, L. S. Breger, *Spacecraft Formation Flying. Dynamics, Control and Navigation , Elsevier Astrodynamics.* 2010.

Fortescue. P. W. and Stark, J. P. W. (ed.), *Spacecraft Systems Engineering.* Wiley. New York, 1991.

Larson, W. J. and Wertz, J. R. (ed.), *Spare Mission Analysis and Design.* Kluwer Academic Publishers, Dordrecht, 1992.

Murphy, R., Pardalos, P.M. (eds.), *Cooperative Control and Optimization*, Kluwer Academic Publishers 2000.

Scharf, D.P., Hadaegh, F.Y., Ploen, S.R., *A Survey of Spacecraft Formation Flying Guidance and Control (Part II): Control*, Proceedings of the 2004 American Control Conference, Boston MA.

Schilling, K., *The use of computer algebra systems to simulate satellites*. In *Mathematics with Vision.* In: V. Keränen and P. Mitic (eds.), Computationa1 Mechanics Publications Southampton. 1995. pp. 333-340.

Schilling, K., *Design of Pico-Satellites for Education in System Engineering*, IEEE Aerospace and Electronic Systems Magazine 21 (July 2006), p. 9-14.

Schilling, K. and Brieß, K. (eds.), *Analyse der Anwendungsfelder und des Nutzungspotentials von Pico- und Nano-Satelliten*, Bericht 50RU0701/2 an die Raumfahrt-Agentur des DLR, 2008.

Schmidt, M., K. Ravandoor, O. Kurz, S. Busch, K. Schilling, *Attitude Determination for the Pico-Satellite UWE-2*, Proceedings IFAC World Congress, Seoul 2008.

Schmidt, M., Schilling, K,. *Formation Flying Techniques for Pico Satellites.* Proceedings 6th International Workshop on Satellite Constellation and Formation Flying, Taiwan 2010.

Sidi, M. J., *Spacecraft Dynamics and Control*, Cambridge University Press, 2001.

Twiggs, R., *The next Generation of Innovative Space Engineers: University Students are Now Getting a Taste of Space Experience Building, Launching and Operating their own Space Experiments with Low-Cost Picosatellites*, Proceedings of the 5th ESA International Conference on Spacecraft Guidance, Navigation and Control Systems 2002, p. 409-422.

Vallado, D.A., *Fundamentals of Astrodynamics and Applications*, McGraw-Hill 1997.

Walker, J.G., *Satellite Constellations*, Journal of the British Interplanetary Society 37 (1984), p.559 – 572.

Wertz, J. R. (cd.), *Spacecraft Attitude Determination and Control,* Kluwer Academic Publishers, Dordrecht, 1978.

Zeiger, F., N. Krämer, K. Schilling, *Parameter Tuning of Rrouting Protocols to Improve the Performance of Mobile Robot Teleoperation via Wireless Ad-hoc Networks*, Proceedings 5th International Conference on Informatics, Automation and Robotics (ICINCO), 2008.